Sedimentology (2008) doi: 10.1111/j.1365-3091.2008.00999.x

Sediment provenance in a tropical fluvial and marine context by magnetic 'fingerprinting' of transportable sand fractions

B. A. MAHER*, S. J. WATKINS*, G. BRUNSKILL†, J. ALEXANDER‡ and C. R. FIELDING§
**Centre for Environmental Magnetism and Palaeomagnetism, Lancaster Environment Centre, University of Lancaster, Lancaster LA1 4YQ, UK (E-mail: b.maher@lancaster.ac.uk)*
†*84 Alligator Creek Road, Alligator Creek, Qld 4816, Australia*
‡*School of Environmental Sciences, University of East Anglia, Norwich, Norfolk NR4 7TJ, UK*
§*Department of Geosciences, 214 Bessey Hall, University of Nebraska-Lincoln, Lincoln, NE 68588-0340, USA*

Associate Editor: Steve Rice

ABSTRACT

The sources and fluxes of sediment to the Great Barrier Reef lagoon from north-eastern Australian rivers have been the subject of much concern and study, with the large catchments of the Burdekin and Fitzroy Rivers thought to be the key sources at present. Here, the utility of newly developed magnetic 'fingerprinting' methods for identifying sediment provenance, both onshore and offshore, and in association with individual large flood events, is investigated. Within the Burdekin catchment, sediments are mobilized from different subcatchments by runoff generated by intense, localized rainfall events. Magnetic measurements were made on untreated and acid-treated samples of river channel sediments within the Burdekin River subcatchments and from the estuarine and inner shelf depocentres of Burdekin River sediments. The acid treatment removes all discrete magnetic particles and coatings, and leaves magnetic inclusions (protected within host silicate grains) as the basis of the measured magnetic signature of a sample. The magnetic properties of the acid-treated samples display statistically distinct sediment provenance groupings. Sand samples from the Upper Burdekin River appear magnetically distinct from samples from tributaries of the Burdekin (e.g. Hann Creek, Fanning River) and also from nearby coastal rivers, including the Haughton. Suspended sand samples from a Burdekin flood event in 2000 appear to have a different source compared with those from floods in 1998 and 1999. Comparisons of the terrestrial, acid-treated sand fractions with the same, acid-treated, sand-size fractions from transects taken offshore suggest that the surface sediments in Upstart Bay and Bowling Green Bay have different sources. Some of these sources are as yet unidentified but may represent the unsampled, lower-discharge south-western Burdekin subcatchments, and/or along-shore drift of sand from the south, perhaps even from the Fitzroy River, over millennial timescales of cyclone pumping. The magnetic inclusion method precludes any obfuscation or confounding of sediment source, which might arise from hydraulic sorting and/or post-depositional magnetic diagenesis or authigenesis.

Keywords Great Barrier Reef, magnetic fingerprinting, magnetic inclusions, sediment provenance, tropical rivers.

INTRODUCTION

The Burdekin catchment and sediment delivery to the Great Barrier Reef

The Burdekin catchment (Fig. 1), NE Australia, covers an area of 130 000 km^2 and is the largest source of sediment to the central Great Barrier Reef (GBR) lagoon (e.g. Belperio, 1983; Neil *et al.*, 2002; Prosser *et al.*, 2002; Furnas, 2003). The catchment, located in the semi-arid tropical region of Queensland, is dominated by short-duration, intense cyclonic rainfall causing sporadic discharge events. Monsoonal rain and smaller-scale tropical depressions also contribute variably across the region. Mean annual rainfall ranges from 500 mm in the Queensland interior to 1200 mm on the humid coastal plain and hills; the most intense rainfall occurs mainly between January and April (Australian Government Bureau of Meteorology; http://www.bom.gov.au/climate). Major discharge events within the lower Burdekin can be generated by intense rainfall over sub-areas of the upper catchment and/or locally on the coastal belt (e.g. Alexander *et al.*, 1999). Annual discharge is extremely variable (2×10^8 to $2{\cdot}9 \times 10^{10}$ m^3), with an annual mean value of $9{\cdot}8 \times 10^9$ m^3 [Queensland Department of Natural Resources and Water (QNRW); http://www.nrw.qld.gov.au/watershed]. During high-discharge events, the Burdekin entrains and transports considerable volumes of sediment. Estimated sediment delivery per year varies from $2{\cdot}7 \times 10^6$ (Moss *et al.*, 1992) to $9{\cdot}0 \times 10^6$ (Neil *et al.*, 2002) tonnes to a small area of the inner continental shelf. The maximum recorded discharge in the Burdekin delta (Home Hill) was 40 392 m^3 sec^{-1} in March 1946; Belperio (1979)

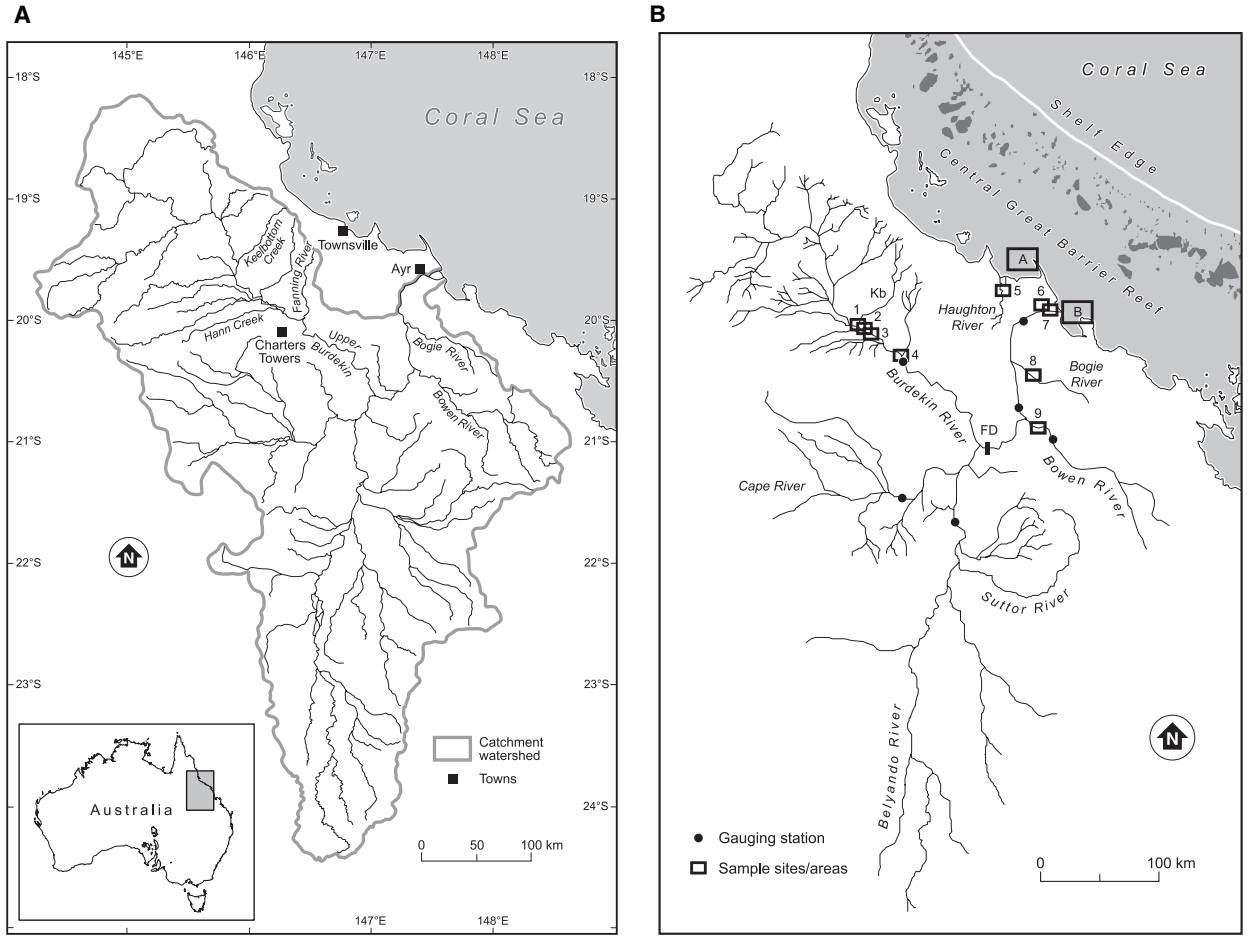

Fig. 1. (A) The Burdekin River catchment, showing the tributaries referred to in this paper and (B) sample sites/areas: FD = the Burdekin Falls Dam, (1) Keelbottom Creek (Kb) confluence with Burdekin River; (2) Upper Burdekin River sites, Big Bend and Brigalow Bend (including samples G1, G2, BB, R. bank); (3) Hann Creek; (4) Fanning River confluence with Burdekin River; (5) Haughton River; (6) Palaeochannels; (7) Burdekin River Delta sites; (8) Bogie River; (9) Bowen River; [A] Bowling Green Bay; [B] Upstart Bay.

estimated that ~8·4 million tonnes of sediment were delivered to the Burdekin delta during this flood event. The Burdekin Falls Dam (impounding Lake Dalrymple) was completed in 1987. More than 80% of the Burdekin catchment area is above the dam (Fig. 1B). Its construction has influenced the discharge characteristics below the dam, decreasing early wet-season discharge in low and intermediate flow events (e.g. Alexander *et al.*, 1999; Alexander & Fielding, 2006) but not significantly affecting major discharge events (consistent with its design criteria). Dry season flow has been increased slightly by irrigation water from the lake but this very low discharge transports insignificant volumes of sediment. The influence of the dam on wet-season sediment loading and transport is uncertain, as there were few pre-dam studies, but it is evident that the dam traps significant proportions of the sediment derived from the upstream north-western portion of the river catchment (Prosser *et al.*, 2002; Amos *et al.*, 2004).

The geology of the Burdekin catchment is diverse (Fig. 2). The southern half of the catchment consists primarily of sedimentary rocks (mostly sandstones, mudrocks and coals) from the Permo-Triassic Bowen and Galilee Basins, with some older Palaeozoic volcanic successions exposed in the south-west. The northern half, thought to be subject to more erosion than the southern section (Prosser *et al.*, 2002), is geologically more complex. It consists mainly of Palaeozoic volcanic, plutonic sedimentary and metasedimentary rocks of the Tasman Orogenic Belt. Tertiary to Recent sediments and basalt flows also occur across large parts of the north-western subcatchment (Fielding & Alexander, 1996; Alexander *et al.*, 2001). In the middle and lower reaches, the channel deposits within the Burdekin and its tributaries are composed mostly of coarse-grained to very coarse-grained arkosic sand with localized deposits of gravel to boulder grade and thin mud drapes (Fielding & Alexander, 1996; Fielding *et al.*, 2005). Fine-grained sand and silt occur on the bank tops and upper vegetated bars, and much of the floodplain deposits are sand (Alexander & Fielding, 2006).

The catchment is dominated by grazing (mainly beef cattle), with small areas where arable agriculture is practised (dominantly sugar cane) on the floodplain and deltaic areas, and some mining. Land use, climate, topography and vegetation cover each has a significant impact on the source and amount of sediment entering the Burdekin River system (e.g. Neil *et al.*, 2002).

Uncertainty exists over the level of sediment input to floodplains, the delta and inner shelf, and the effect of this sediment on the mid-shelf reefs (e.g. Brodie, 1996; Larcombe *et al.*, 1996; Cavanagh *et al.*, 1999; Larcombe & Woolfe, 1999; Orpin *et al.*, 1999; Pringle, 2000; Neil *et al.*, 2002; Prosser *et al.*, 2002; Alibert *et al.*, 2003; McCulloch *et al.*, 2003). The total Holocene sediment mass held within the Burdekin Delta, calculated from the isopach map of Fielding *et al.* (2006) suggests that nearly all the Holocene sediment delivered by the river to the coast (using estimated modern annual sediment yields; Fielding *et al.*, 2006) has been stored in the delta, rather than being dispersed into the Great Barrier Reef shelf. Nonetheless, when the flow of the Burdekin River exceeds ~2000 m^3 sec^{-1}, a turbid plume is visible on the inner shelf, extending up to 10 km offshore (Belperio, 1983; Wolanski, 1994). Suspended sediment from the plume is transported north-westward by currents driven by prevailing winds and waves (Wolanski, 1994). Fluvial sediment fluxes are thought to have increased in the order of two to eight times since European settlement (Johnson, 1996; Larcombe *et al.*, 1996; Cavanagh *et al.*, 1999; Neil *et al.*, 2002; Prosser *et al.*, 2002; Alibert *et al.*, 2003; McCulloch *et al.*, 2003); this has been attributed to increased soil erosion through land-use change, resulting particularly from forest clearance and increased grazing and arable agriculture (Cavanagh *et al.*, 1999). This increase may adversely impact key marine environments along the inner continental shelf, including inshore coral, mangrove and sea grass communities. However, baseline and even contemporary information on changes in sediment loading and/or in sediment source remains scarce, which is unsurprising given the large size of the Burdekin catchment, and the complex interplay among episodes of drought and floods, sediment supply, sediment storage and transport, hydrodynamics and local geology and geomorphology. If soil loss rates are significant and there is a threat to the GBR lagoon by increased sediment influx, then two key requirements emerge: (i) identify those subcatchment areas most at risk of accelerated erosion; and (ii) mitigate at sediment source. This study tests and demonstrates one feasible approach to the former.

The Burdekin catchment is composed of the Upper Burdekin subcatchment (~28% of the total area), the Cape River subcatchment (12%), the Belyando-Suttor subcatchment (38%) and the Bowen-Broken subcatchment (7%). Although

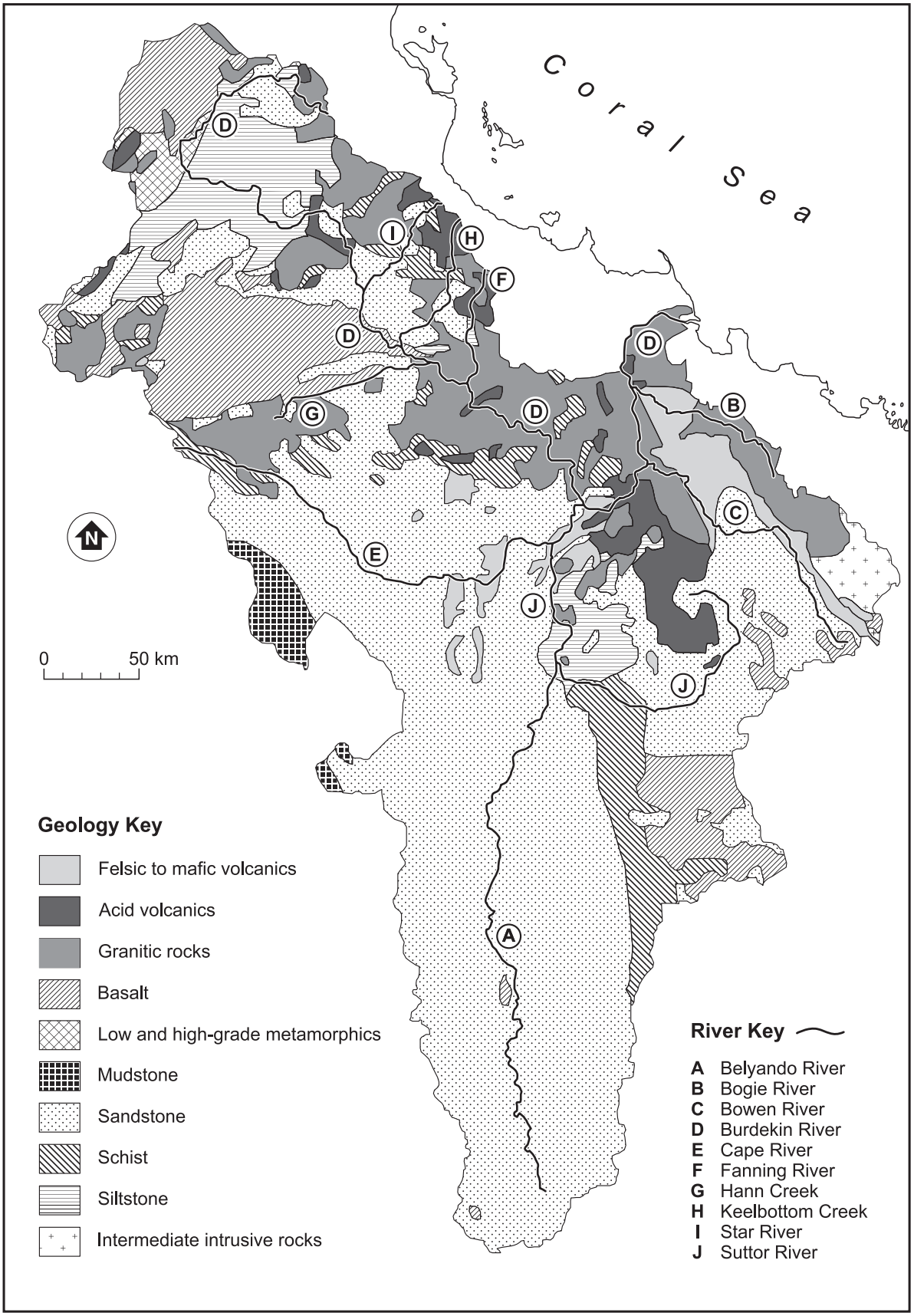

Fig. 2. Map showing the distribution of lithologies across the Burdekin River catchment.

the Upper Burdekin subcatchment represents only about 28% of the area, it generates ~43% of the mean annual discharge (calculated from QNRW data), though, in individual discharge, its contribution varies considerably (from ~0 to 100%). This variation reflects the higher rainfall experienced by the eastern parts of the catchment, the Upper Burdekin and Bowen-Broken River subcatchments. In contrast, the more arid Belyando-Suttor subcatchment generally contributes relatively less to the total runoff (~14% to 18%; calculated from QNRW data).

Within the Burdekin catchment itself, sedimentological and hydrological processes and fluvial geochemistry have been studied in detail (e.g. Alexander & Fielding, 1997, 2006; Alexander *et al.*, 1999, 2001; Nakayama *et al.*, 2002; Prosser *et al.*, 2002; Amos *et al.*, 2004; Fielding *et al.*, 2005, 2006). Despite these numerous studies, sediment sourcing within the catchment has so far received relatively little attention. Cavanagh *et al.* (1999) measured organochlorine residues in soils of the Burdekin coastal plain, but these were undetectable in sediments of Upstart and Bowling Green Bay, suggesting that soil erosion from this zone might occur at rates slower than anticipated. For the Burdekin, Prosser *et al.* (2002) suggest that spatial modelling is the only practical framework for assessing patterns of sediment transport across such a large and complex area. The Prosser *et al.* reconnaissance-level spatial modelling suggests that hillslope erosion is the dominant process (reflecting high rainfall erosivity and often low vegetation cover, resulting from drought and/or over-grazing pressure), with 95% of sediment exported to the delta coming from only 13% of the catchment, mainly located in the north and north-east. Their sediment budget predicts that only 16% of suspended sediment delivered to the river network in any one year is exported to the river mouth and beyond. Of this sediment, the Prosser *et al.* models suggest that 85% comes from the eastern parts of the catchment, from parts of the Upper Burdekin subcatchment and areas draining into the Burdekin downstream of the Burdekin Falls Dam including the Bowen River basin. As for any modelling approach, validation of modelled results is essential and they do provide testable hypotheses regarding the major sources of suspended sediment through the Burdekin catchment. Data that go some way towards testing this model output are presented.

The aims of this study were to address three key questions: (i) Can sediment provenance, onshore and offshore, be identified magnetically even in a catchment as large and complex as the Burdekin? (ii) Can provenance information be gained on the large, individual flood events which characterize the flashy, tropical hydrology of this region? (iii) What are the advantages and disadvantages of using the magnetic inclusion approach either to replace or complement whole-sample magnetic fingerprinting?

Application of environmental magnetic techniques to sediment provenance

Direct methods of sediment sourcing include magnetic 'fingerprinting' of discrete subcatchment soils, suspended sediments and channel sediments (e.g. Oldfield *et al.*, 1979, 1985; Walling *et al.*, 1979; Walling & Woodward, 1995; Walden *et al.*, 1997; Caitcheon, 1998a,b). So far, however, this approach has been applied to river catchments which are significantly smaller and less complex than the Burdekin. Here, magnetic methods have been used to examine whether it is possible to differentiate fluvial sediments sourced from different subcatchments of the large system of the Burdekin River. The magnetic properties of sediments most often vary according to the characteristics of the magnetic minerals they contain – their mineralogy, concentration, magnetic domain state, morphology and composition. Minerals capable of acquiring magnetic remanence include mainly the iron oxides (magnetite, maghemite and hematite), oxyhydroxides (goethite) and sulphides (greigite). Magnetic iron sulphides are found only in reducing (anoxic) environments, such as estuarine muds, where organic matter is consumed by bacteria in the absence of oxygen. The strongest naturally occurring magnetic minerals are magnetite and maghemite, while hematite and goethite are magnetically much weaker. These four minerals occur virtually ubiquitously throughout the natural environment. These minerals can occur as discrete particles, ranging in size from millimetres to nanometres (Fig. 3A to C), as coatings on other particles and as particles included within host grains (Fig. 3D). Volumetrically, these minerals most often occur as only minor (in the case of hematite and goethite) or trace (in the case of magnetite) components of samples. However, these minor or trace magnetic components can carry key environmental information because their characteristics, or magnetic 'signature', vary according to their source and depositional history. Furthermore, sensitive magnetic measurements

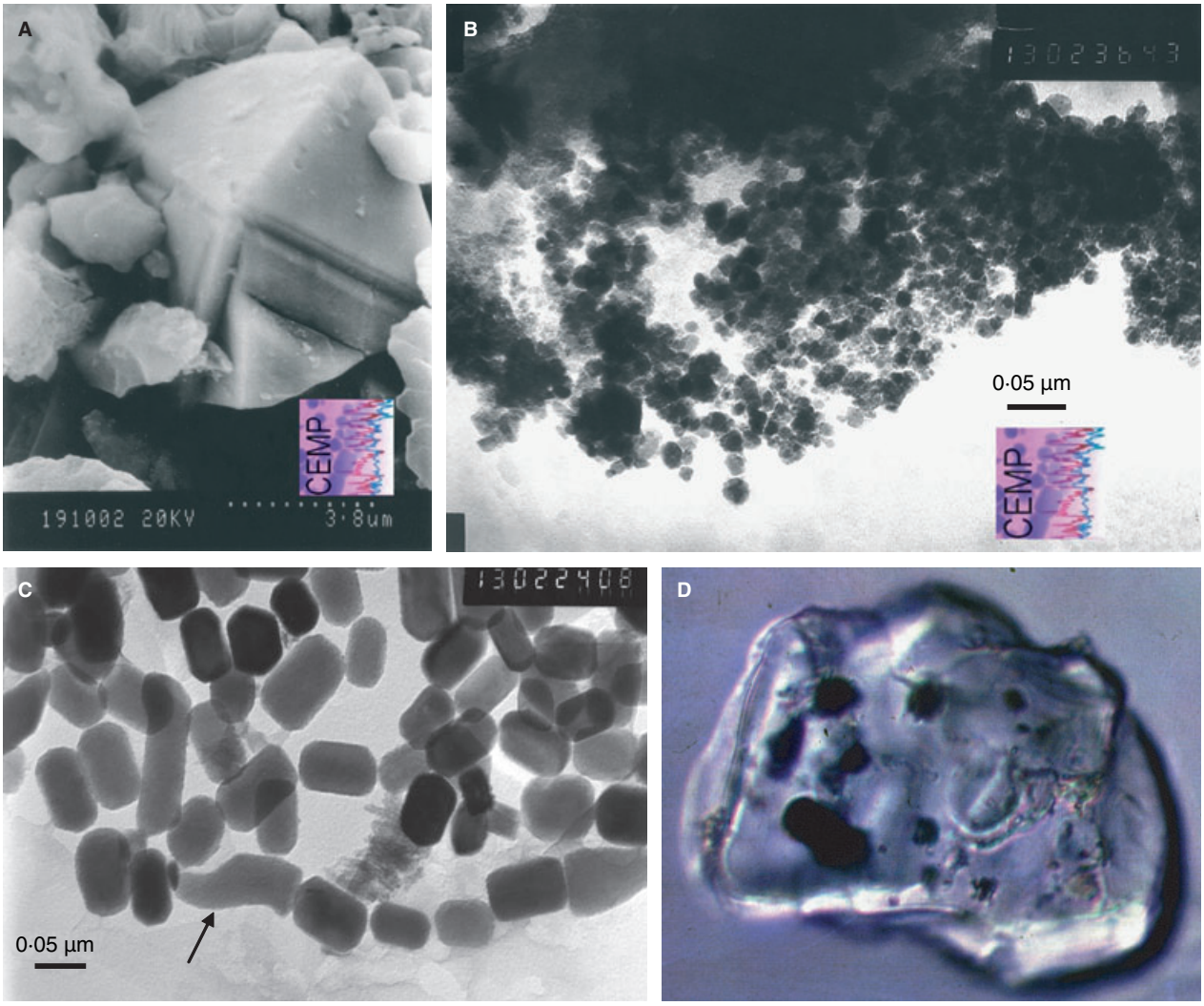

Fig. 3. Electron micrographs of different types of natural magnetic particles: (A) detrital lithogenic titanomagnetite, ~5 μm, from aeolian loess (Chinese Loess Plateau); (B) submicrometre, soil-formed magnetite from a soil in SW England; (C) submicrometre, bacterially formed magnetite (note the boot-shaped crystal, arrowed, a unique crystal habit diagnostic of intracellular bacterial origin); (D) magnetic inclusions within a host quartz grain, Coral Sea sediments (width of micrograph = 25 μm).

(i.e. to concentrations of less than one part per million for weakly magnetic minerals like hematite and less than one part per billion for strongly magnetic minerals like magnetite) can be made relatively cheaply and rapidly compared with other types of mineralogical analysis.

Table 1 provides a summary of magnetic measurements used routinely in environmental magnetic studies and describes what they indicate about the magnetic minerals present in a sample. Figure 4 illustrates the magnetic response of a sample to a series of laboratory-generated magnetic fields and identifies many of the magnetic parameters referred to here. Maher *et al.* (1999) provide an overview of environmental magnetic minerals, measurements and magnetic applications within a range of Quaternary contexts.

Using these different magnetic measurements, absolute, sample mass-normalized values (magnetic susceptibility, saturation remanence) can be used to identify changes in magnetic mineral concentration, and various magnetic ratios can be used to assess changes in magnetic grain-size. Because magnetic measurements can be performed quite quickly and easily, it is possible to assess the major magnetic contributions and characteristics of reasonably large numbers of samples (e.g. hundreds to thousands) and to use these characteristics to differentiate between samples. Critically, within the Burdekin catchment,

Table 1. Short summary of environmental magnetic parameters and instrumentation.

Magnetic susceptibility, (normalized to sample mass) *Magnetic concentration*	The ratio of magnetization induced in a sample to the intensity of the magnetizing field. Measured *within* a small AC field (~0·1 mT, ~2·5× the magnetic field of the Earth) and is reversible (i.e. no magnetic remanence is induced). Roughly proportional to the concentration of strongly magnetic (e.g. magnetite-like) minerals. Weakly magnetic minerals, like hematite, have much lower susceptibility values; water, organic matter have negative susceptibility. *Instrumentation* single sample susceptibility meter *Units* $m^3\ kg^{-1}$
Anhysteretic remanent magnetization, ARM or anhysteretic susceptibility, χARM *Ultrafine magnetite*	If a sample is subjected to a decreasing AC field with a small DC field superimposed, it acquires an anhysteretic remanence. ARM is sensitive both to the concentration and grain size of ferrimagnetic (magnetite-like) grains, highest for grains close to the lower single domain (SD) boundary and lowest for coarse multidomain (MD) magnetic grains (e.g. > ~5 μm in magnetite). If ARM normalized for the DC field strength (desirable as different laboratories use different DC fields), it is termed an anhysteretic susceptibility. *Instrumentation* anhysteretic magnetizer (max. AC field 100 mT, DC field often ~0·08 mT); fluxgate magnetometer. *Units* ARM, A m^2, χARM $m^3\ kg^{-1}$
Saturation remanence, SIRM *Magnetic concentration*	The highest level of magnetic remanence that can be induced by application of a 'saturating' magnetic field (in many laboratories the highest DC field is 1 T, sufficient to saturate magnetite but not hematite or goethite). SIRM is an indicator of the concentration of magnetic minerals in a sample but also responds (albeit less sensitively than ARM) to magnetic grain-size. *Instrumentation* pulse magnetizer and/or electromagnet; fluxgate magnetometer
Remanence ratios, IRM_{nmT}/SIRM %, *Degree of magnetic 'softness' or 'hardness' (MD vs. SD magnetite; magnetite vs. hematite)*	A 'soft' mineral (e.g. coarse MD magnetite) will acquire remanence easily, at low fields (e.g. IRM_{20mT}/SIRM of 90%; a 'hard' mineral (e.g. hematite) will magnetize only at high fields (e.g. IRM_{20mT}/SIRM of <5%, IRM 300 mT/SIRM of ~30%)

sediments are mobilized from different subcatchments by runoff generated by intense, localized rainfall events. Sediment samples from subcatchments with different geology, climate and land use were collected and analysed to test whether their magnetic properties vary with provenance.

This paper presents a pilot study of magnetic 'fingerprinting' of Burdekin, and associated tributary, river-bed and offshore samples, using a novel magnetic tracing method based, firstly, on measurements of the (untreated) transportable sand fraction (250 to 355 μm) and, secondly, this size fraction after acid dissolution. The acid dissolution procedure removes any discrete magnetic particles or coatings in this fraction, leaving only those magnetic particles which exist as inclusions protected within host silicate particles (e.g. Fig. 3D). The rationale behind this approach is three-fold and is designed to optimize the robustness of the magnetic tracer. Firstly, discrete magnetic particles in the untreated sand fraction may be denser than the majority of the silicates present and may thus exhibit hydraulic sorting effects. Secondly, post-depositional reductive dissolution of discrete magnetic particles can occur, especially in offshore anoxic zones (e.g. Karlin and Levi, 1985, and possibly in the lower reaches and the delta plain, as a result of acidic soil pore waters, with the result that at least part of the magnetic tracer signal might be erased. Thirdly, *in situ*, post-depositional formation of bacterial magnetite (see, e.g. Fig. 3C; Blakemore *et al.*, 1984; Bazylinski, 1990) can also 'overprint' any original sediment magnetic signatures. In order to avoid all these problems, all the discrete magnetic particles are removed by acid pretreatment (Alekseeva & Hounslow, 2004; Hounslow & Morton, 2004). Any bacterial magnetite is also removed by dissolution. After all these procedures, the remaining sediment magnetic properties are only those of magnetic particles occurring as inclusions within host silicate

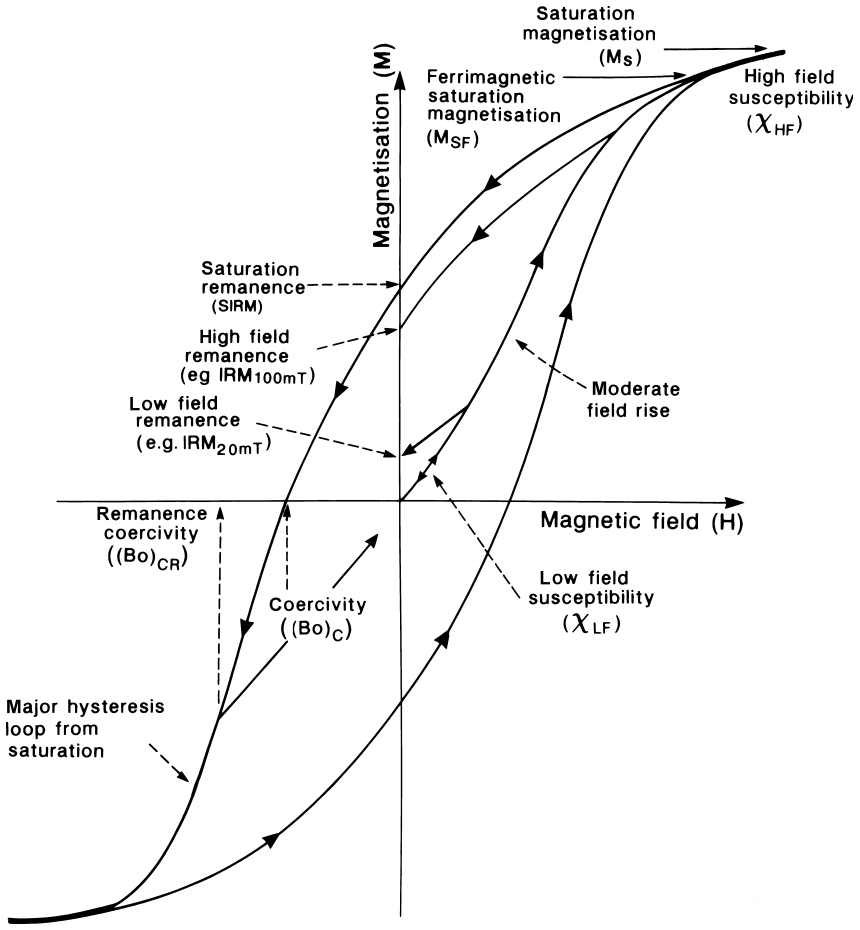

Fig. 4. Magnetic hysteresis loop, showing some of the magnetic parameters routinely used in environmental magnetic studies, including in-field measurements (e.g. magnetic susceptibility) and remanent measurements (e.g. ARM, SIRM and various remanence ratios, such as the 'soft' remanence, $\%IRM_{0–20mT}$, 'intermediate' remanence, $\%IRM_{50–100mT}$, 'hard' remanence, $\%IRM_{100–300mT}$, and 'hardest' remanence, $IRM_{300–1000mT}$). From Maher *et al.*, 1999.

grains, especially quartz and feldspars (Hounslow and Maher, 1996). Such magnetic inclusions are both hydrodynamically representative and protected from post-depositional attack by reductive diagenesis.

METHODOLOGY

Large amounts of sand are transported during moderate-flow and high-flow events both in suspension and as bedload, with continuous interchange between the two loads (Amos *et al.*, 2004). Even at only moderate discharge, medium-grade sand is found in suspension in the water column. The consequence of this highly dynamic sediment transport is that medium-grained sand is deposited from bed or suspended load in a wide range of environments (in channels, floodplains and beyond the channel mouth) and, thus, by considering only this grain-size fraction, the effects of hydraulic sorting (which might otherwise mask provenance patterns) are overcome.

Fifty-seven sand samples were collected from locations (Fig. 1A and B) along the Upper Burdekin River, from a number of tributaries and subcatchments (Bowen, Bogie and Fanning Rivers and Keelbottom and Hann Creeks) and from the Haughton River and its tributary, the Reid River. Four samples were collected from palaeo-channels on the delta plain. Twelve suspended load samples were obtained from the Burdekin River on the delta during three flood events (1998, 1999 and 2000) and four mid-channel mobile bedload samples were collected in 2000 using a winch-mounted Helley-Smith sampler (Rickly Hydrological Company, Columbus, OH, USA). The suspended sediment samples were obtained by pumping flood-stage surface water into 200 l barrels and a 1000 l tank in the middle of a bridge. The samples in these closed barrels and tanks were left to settle in the shade for several days, after which the supernatant was syphoned away, and the settled sediment was washed into a 4 l container. This slurry of sediment was then centrifuged and the sediment plug freeze-dried.

In addition, a series of sediment samples was obtained from the inner continental shelf adjacent to the Burdekin delta, using a heavily weighted

Van Veen Smith-MacIntyre grab sampler (Australian Institute of Marine Science, Townsville, Australia) aboard the *R/V The Harry Messel*, on Australian Institute of Marine Sciences (AIMS) cruises between 1994 and 1998. Two shore-normal transects of samples from 3 to 50 m water depth were analysed here, spanning Upstart Bay and Bowling Green Bay.

Untreated samples were sieved to obtain the medium sand fraction (250 to 355 μm). After drying at 40 °C, samples were weighed to allow for correction of all magnetic measurements to a dry mass-specific basis. A suite of magnetic measurements was first performed on this otherwise untreated sand fraction with the aim of characterizing magnetic mineralogy, concentration and magnetic domain state and thus, indirectly, magnetic grain-size (see *Appendix*). After this initial magnetic characterization, organic material was removed using 30% hydrogen peroxide solution. An acid dissolution procedure (37% hydrochloric acid) was then used to remove all discrete iron oxide or sulphide particles, leaving only magnetic inclusions within the host silicate grains to provide the measured magnetic signature. These inclusion-based samples were subjected to the same magnetic measurements as the untreated samples, with the exception that they were too weak to be measured on the Molspin magnetometer (Molspin Ltd, Newcastle, UK) and remanences were measured instead on a more sensitive magnetometer (an AGICO JR-6A dual-speed spinner magnetometer (AGICO Inc., Brno, Czech Republic), ~10 times the sensitivity of the Molspin magnetometer).

Having obtained these multi-parameter magnetic data sets, two multivariate statistical methods were applied to robustly characterize and/or differentiate the sediments; cluster analysis (using fuzzy c-means) and non-linear mapping, using the program of Vriend *et al.* (1988). Both techniques have been applied successfully to a number of environmental data sets (e.g. Vriend *et al.*, 1988; Dekkers *et al.*, 1994; Kruiver *et al.*, 1999; Schmidt *et al.*, 1999; Hanesch *et al.*, 2001; Watkins & Maher, 2003). Five key, diagnostic, magnetic parameters (see Table 1) were selected for use in the cluster analysis of the inclusion data set. Magnetic susceptibility indicates the magnetic mineral concentration; and anhysteretic remanent magnetization (ARM; normalized to the saturation remanence, to remove any concentration dependence) indicates the presence of ultrafine-grained magnetite. Three isothermal remanent magnetization/saturation isothermal remanent magnetization (IRM/SIRM) ratios were also included to identify differences in magnetic 'hardness': the percentage of IRM acquired in moderate applied fields (between 50 and 100 mT, $\%IRM_{50–100mT}$), higher fields (between 100 and 300 mT, $\%IRM_{100–300mT}$) and high fields (between 300 and 1000 mT, $\%IRM_{300–1000mT}$). Prior to cluster analysis, the parameters were tested for autocorrelation using the non-parametric Spearman test. Outliers (values more than three times the standard deviation from the mean; here, seven samples only) were removed from the data set, to avoid formation of unrealistic cluster groupings (Hanesch *et al.*, 2001) and values were standardized so that parameters with large values and/or variability do not dominate. Initial cluster memberships are randomly defined; the 'best' solution is then calculated by minimizing the distance between a sample and its cluster centre and maximizing the distance between the cluster centres. Two statistics represent those distances, the partition coefficient, F, and the classification entropy, H (Vriend *et al.*, 1988); optimal clustering is indicated when F is high (closest to 1) and H is low (closest to 0). Non-linear mapping (NLM) additionally was used to examine data groups, by scaling and calculating the distance between data points in multi-dimensional space, then translating this into two dimensions (Vriend *et al.*, 1988).

RESULTS

Burdekin River sand samples

Figure 5A shows an overview (optical micrograph) of the untreated medium sand fraction (250 to 355 μm) from the Upper Burdekin River channel, with discrete opaque iron oxide particles seen admixed within the dominant silicate mineralogy. Figure 5B shows the presence of magnetic particles occurring as inclusions within a host quartz grain; these inclusions are the only remaining magnetic contributors after application of the acid dissolution treatment. The untreated sediments from different reaches and tributaries of the Burdekin display different magnetic properties. For example, in terms of magnetic susceptibility and saturation remanence (both reflecting mainly the concentration of magnetic minerals in the sediment), the sand samples from the Upper Burdekin River (the Big Bend and Brigalow Bend reach) are much more magnetic (susceptibility of ~20 to 30×10^{-8} m^3 kg^{-1}, saturation remanence ~2000 to 9700×10^{-6} A m^2 kg^{-1}) than those from either the

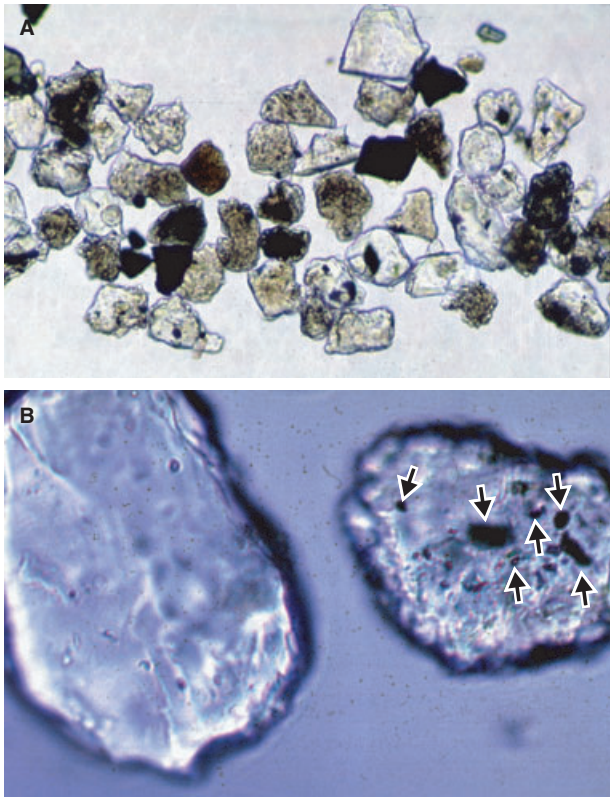

Fig. 5. (A) Untreated medium sand fraction from the Burdekin River, with discrete opaque magnetic grains among the more dominant quartz and feldspars; (B) magnetic inclusions (e.g. see arrowed grains) within host silicates after acid dissolution treatment of the medium sand fraction.

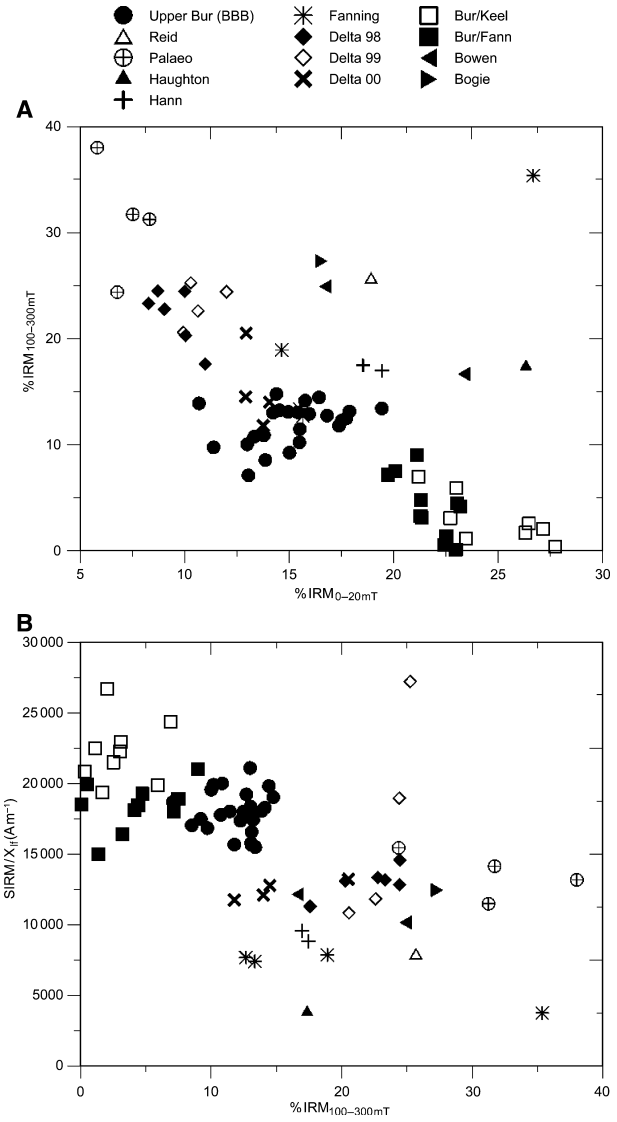

Fig. 6. (A) Untreated medium sand fraction, 'hard' remanence (% of remanence acquired between 100 and 300 mT or $\%IRM_{100–300mT}$) vs. 'soft' remanence (% of remanence acquired between 0 and 20mT or $\%IRM_{0–20mT}$). BBB, Big and Brigalow Bends; (B) untreated medium sand fraction, $SIRM/\chi_{lf}$ vs. 'hard' remanence, $\%IRM_{100–300mT}$.

Fanning River or Keelbottom Creek confluences (susceptibility of $< 1 \times 10^{-8}$ m^3 kg^{-1}, saturation remanence of $\sim$130 to 250×10^{-6} A m^2 kg^{-1}). These higher magnetic concentrations in the Upper Burdekin River samples are likely to reflect the contribution of basalt-derived magnetic grains to these sediments. The samples with the highest values of high-field remanence, indicating the presence of hard, hematite-like minerals, are those from Hann Creek, with 12% of their remanence acquired in fields beyond 300 mT. This observation compares with values mostly less than 5% for the Upper Burdekin River samples.

Plotting one magnetic parameter against another (e.g. Fig. 6A and B) leads to the identification of other differences, arising either from the presence of differing magnetic minerals and/or differing magnetic grain-sizes. For example, for the 'soft' remanence (the percentage of remanence acquired at low applied fields, between 0 and 20 mT) and an 'intermediate' remanence (the percentage IRM acquired between 100 and 300 mT), samples from the Big Bend and Brigalow Bend areas of the Upper Burdekin River plot in a well-defined group, with moderate values for both these remanence ratios (Fig. 6A). Samples from the Burdekin upstream and downstream of the Fanning River and Keelbottom Creek confluences (Fig. 1) are distinct both from the Big Bend and Brigalow Bend samples and samples from other areas of the catchment and delta. These samples have lower $\%IRM_{100–300mT}$ but higher $\%IRM_{0–20mT}$ values, indicating a greater contribution from 'soft', easily magnetized magnetite. In contrast, the flood event samples

collected from the Burdekin delta have higher $\%IRM_{100–300mT}$ and lower 'soft' $\%IRM_{0–20mT}$ values; they thus have a greater contribution from 'harder' magnetic minerals, such as single domain-like magnetite or the much 'harder' mineral, hematite. The 1998 and 1999 flood event samples are magnetically alike, while the 2000 event samples have a slightly higher $\%IRM_{0–20mT}$ and lower $\%IRM_{100–300mT}$. The palaeo-channel samples from the delta plain are also quite distinct; they display the lowest $\%IRM_{0–20mT}$ (i.e. little coarse-grained, 'soft' magnetite) and highest $\%IRM_{100–300mT}$ values (indicating more, 'harder', single domain-like, ferrimagnets and/or some 'hard' hematite or goethite). In a similar fashion, Fig. 6B shows the grouping of samples when the saturation remanence/susceptibility ratio is used for testing the magnetic discrimination. Again, the Big Bend and Brigalow Bend samples group quite tightly and separately, as do the samples from the Fanning River and Keelbottom Creek confluences. Similarly, the Hann Creek samples plot close together and separately from other samples. The delta samples (channel bed and flood events) and Fanning River samples are distributed more widely.

While this initial discrimination of the untreated sand samples appears promising, it is possible that some of the observed variation could be the result of post-depositional processes, e.g. by diagenetic or authigenic alteration of the discrete magnetic grains or by their hydraulic sorting. The magnetic inclusion-based data set removes any possible influence of such confounding factors.

The magnetic biplot for the acid-treated sand fraction (Fig. 7), with its magnetic properties arising only from magnetic inclusions, shows similar groupings to those observed for the untreated data set (Fig. 6), albeit with a more restricted range. The Upper Burdekin River (Brigalow Bend and Big Bend) samples remain distinctive and tightly grouped, with the highest 'harder' remanence ($\%IRM_{100–300mT}$) of any samples. Samples from the Keelbottom Creek and Fanning River confluences remain reasonably well-grouped, with higher 'soft' remanence ($\%IRM_{0–20mT}$) and lower 'harder' remanence ($\%IRM_{100–300mT}$) than the Brigalow and Big Bend samples, indicating a greater contribution from larger, multidomain-like magnetic grains. While the 1998 and 1999 flood event samples remain similar to each other, the 2000 event samples are separated from them, possibly reflecting a different sediment source. The palaeo-channel samples

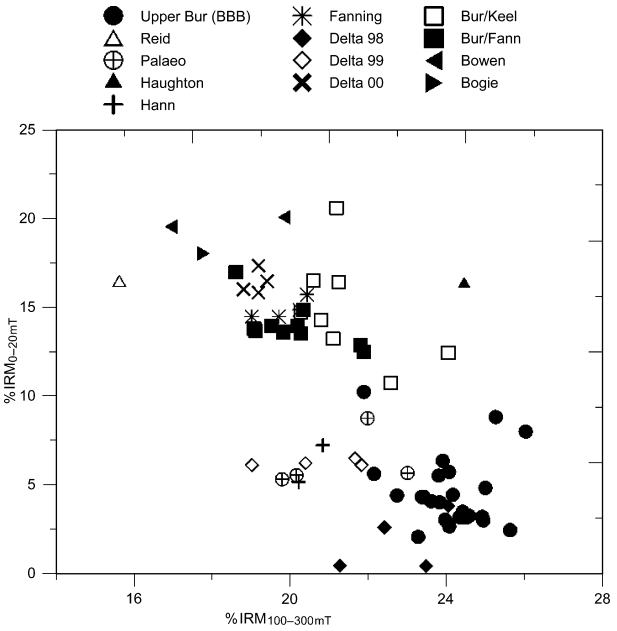

Fig. 7. Treated medium sand fraction (magnetic inclusion-based), 'soft' remanence (% $IRM_{0–20mT}$) vs. 'hard' remanence ($\%IRM_{100–300mT}$). BBB, Big and Brigalow Bends.

are not as distinct as the untreated samples and samples from the other tributaries and rivers narrow in their distribution.

These magnetic biplots indicate that the distinctive groupings of sediments from different subcatchments of the Burdekin remain after the acid treatment of the sand samples. Magnetic discrimination of the different sediment sources can be optimized by making multi-dimensional use of the magnetic data. Cluster analysis (fuzzy c-means cluster analysis) was carried out using five diagnostic magnetic parameters. Statistically, the best cluster solution occurs with five clusters. To examine the sample groupings, the multi-dimensional data can be projected onto a two-dimensional plot, the so-called 'non-linear map' (Fig. 8A). The non-linear map shows that these clusters are statistically distinct and well-separated from each other; within each of the clusters, the majority of samples have very high membership values to that cluster (Fig. 8B). Only samples at the edge of the clusters show any mixing between adjacent clusters.

Most of the samples from Big and Brigalow Bends belong to Cluster Five. Cluster Five has moderate values of magnetic susceptibility (moderate magnetic concentration) and the lowest χ_{ARM}/SIRM (lowest ultrafine magnetite contribution) of any of the clusters (Table 2). It also has the highest 'intermediate' and 'harder' remanence

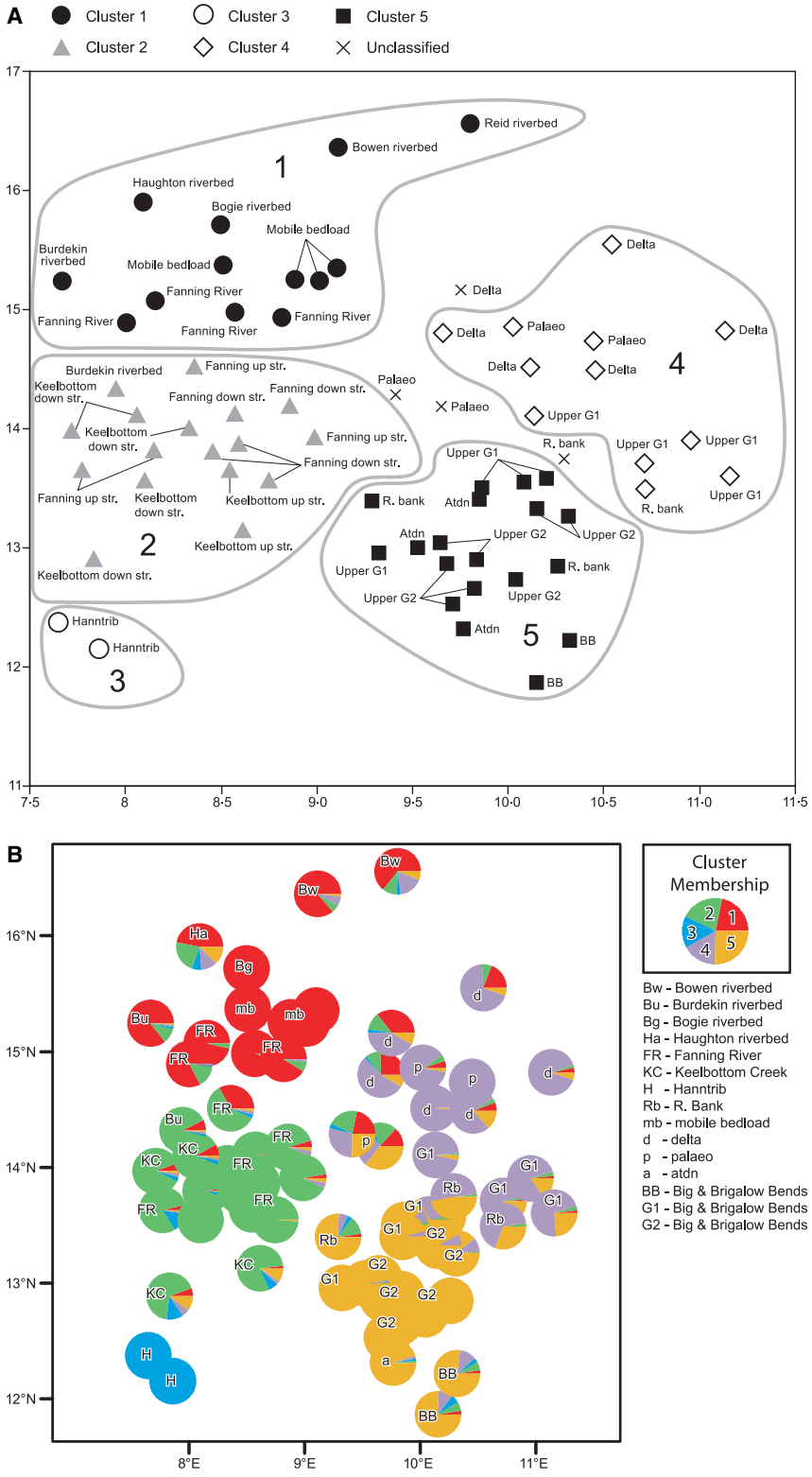

Fig. 8. Non-linear map (NLM) of the five-cluster solution for the medium sand magnetic inclusion data set: (A) with each sample attributed to its dominant cluster; (B) showing the degree of affinity of each sample to each of its possible (fuzzy) clusters.

ratios (%$IRM_{50–100mT}$ and %$IRM_{100–300mT}$). These values suggest that this cluster is dominated by magnetite/maghemite inclusions of intermediate grain-size (~1 μm). Five of the more peripheral Big and Brigalow Bend samples belong to Cluster Four. Cluster Four is composed predominantly of the palaeo-channel samples and 1998 and 1999 flood event samples. It has higher magnetic

Table 2. Parameter means for the five-cluster solution, treated Burdekin River sand (magnetic inclusion) data set.

	Cluster 1	Cluster 2	Cluster 3	Cluster 4	Cluster 5
Susceptibility (10^{-8} m^3 kg^{-1})	2·00	0·62	0·38	1·60	1·04
χ_{ARM}/SIRM (10^{-5} A m^{-1})	113·71	85·56	66·47	76·96	57·24
$\%IRM_{50–100mT}$	27·57	28·85	31·42	34·76	35·25
$\%IRM_{100–300mT}$	19·20	20·60	20·62	22·53	24·10
$\%IRM_{300–1000mT}$	6·09	6·87	11·69	3·49	6·79

susceptibility and ultrafine magnetite (χ_{ARM}/SIRM) values than Cluster Five. Cluster Four also has a much lower value for the 'harder' and 'hardest' remanence ratios ($\%IRM_{100–300mT}$ and $\%IRM_{300–1000mT}$), the lowest of any of the clusters. This cluster thus has the smallest contribution from hematite-like mineral inclusions. The two Hann Creek samples form Cluster Three. This cluster has the lowest susceptibility of any of the clusters and the highest 'hardest' remanence ($\%IRM_{300–1000mT}$), indicating little contribution from magnetite and instead a significant contribution from high-coercivity, hematite or goethite inclusions. Cluster Two consists of all the Burdekin samples upstream and downstream of the Fanning River and Keelbottom Creek confluences. Compared with Cluster Three, it has slightly higher susceptibility and ultrafine magnetite (χ_{ARM}/SIRM) values but lower values of 'moderate' and 'hardest' remanence ($\%IRM_{50–100mT}$ and $\%IRM_{300–1000mT}$). The remaining cluster, Cluster One, contains samples from the other major tributaries and adjacent rivers (Fanning, Bowen, Reid, Haughton and Bogie) and the 2000 flood event samples. Cluster One has the highest magnetic concentration (highest magnetic susceptibility values) and highest contribution from ultrafine magnetite grains (highest χ_{ARM}/SIRM values) of any of the clusters. It is notable that the 2000 flood event samples are well-separated from the 1998 and 1999 flood samples, suggesting a different sediment source in the 2000 event on the delta.

Inner shelf and marine sediments

Given that medium sand fractions from different subcatchments and rivers display distinctive magnetic inclusion-based properties, reflecting differences in their source geologies, it may be possible to apply this magnetic provenancing approach to sand-sized sediments exported to the offshore zone. The magnetic properties of acid-treated, medium sand fractions from two shore-normal grab sample transects across Upstart Bay and Bowling Green Bay were measured. Table 3 shows the particle size distributions (and water depths) for these offshore samples. Beyond the ~20 m depth contour, increasing amounts of biogenic carbonate sand and gravel contribute to the sediments but the terrigenous sand fraction remains the dominant particle size fraction in many of the grab samples (see the carbonate-free sand proportions in Table 3). However, the terrigenous particles seaward from the 20 m depth contour could be either modern or relict Pleistocene in source function age (Belperio, 1983; Orpin & Ridd, 1996; Orpin *et al.*, 1999, 2004; Larcombe & Carter, 2004).

Table 3. Particle size distribution and water depth, grab sample transects, Bowling Green and Upstart Bays (from Orpin *et al.*, 2004).

Grab sample ID	Clay %	Silt %	Sand %		Water depth (m)
BGB901	7	18	75	cf	43
BGB902	8	10	81		40
BGB903	5	6	89		37
BGB904	2	3	95		32
BGB905	8	8	84		30
BGB906	6	6	87		28
BGB907	6	6	88		26
BGB908	9	8	83		25
BGB909	7	29	64	cf	23
BGB718	9	17	73	cf	22
BGB717	9	6	84		19
BGB715	34	18	48		18
BGB713	45	23	32		17
BGB705	3	2	95		5
BGB707	0·2	0·8	99	cf	2
BGB709	0·9	1	98		1
USB981	3	8	89	cf	51
USB978	4	6	89		37
USB977	3	5	92		41
USB976	4	6	90		40
USB974	11	9	80		33
USB973	10	9	81		29
USB972	21	20	59		26
USB970	31	23	46		24

cf, carbonate-free.

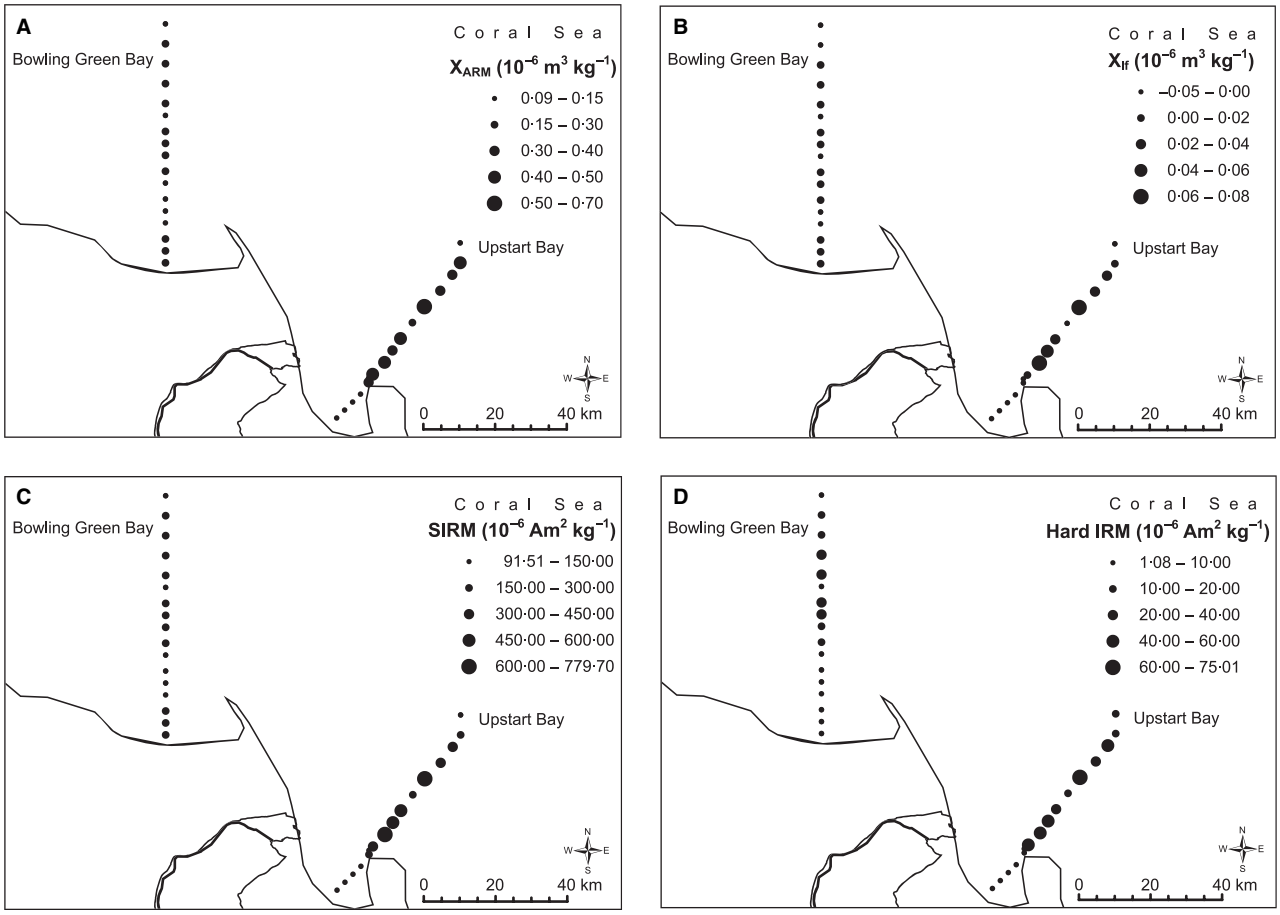

Fig. 9. Concentration-dependent parameters for inclusions within the medium sand fraction of the offshore grab samples.

The sands in Upstart Bay are significantly more variably and strongly magnetic (up to four times more magnetic) than those in Bowling Green Bay, as shown by susceptibility and saturation remanence (Fig. 9). Further contrast between the two bays is seen in both the 'soft' and 'hardest' remanence data (Fig. 10). In particular, the Upstart Bay sands display values of 'hardest' remanence ($IRM_{300–1000mT}$), up to three times higher than the Bowling Green Bay sands, indicating a much greater contribution from high-coercivity hematite-like or goethite-like inclusions. The Bowling Green Bay sands show a trend to increased high-field remanence values offshore. Further contrast between the bays is seen in the ultrafine magnetite (χ_{ARM}/SIRM) values. The sands in Upstart Bay show a mix of very low and very high χ_{ARM}/SIRM ratio values (Fig. 10), higher χ_{ARM}/SIRM ratios indicating the presence of ultrafine ($< \sim 0{\cdot}03$ μm) magnetic inclusions. The Bowling Green Bay sands are less variable and in the middle range of values, with a trend towards decreased values offshore.

These data show that the medium sand fractions within the two bays have different magnetic inclusion-based properties. The use of inclusions, rather than discrete magnetic particles, means that these differences cannot be accounted for by post-depositional diagenesis. Moreover, because the inclusions are contained within one grain-size fraction from the dominant terrigenous silicate particles, the differences cannot be accounted for by hydraulic sorting. Thus, these data suggest that the bays receive medium sand from different sources at the 'present day', or, more strictly, the time period integrated by the grab samples. This time period is dependent upon sediment accumulation rate and the thickness of the sediment mixed layer. In Bowling Green Bay, grab samples probably represent sediments deposited in the last decade or less, whereas grab samples in Upstart Bay may be a composite of at least the last century

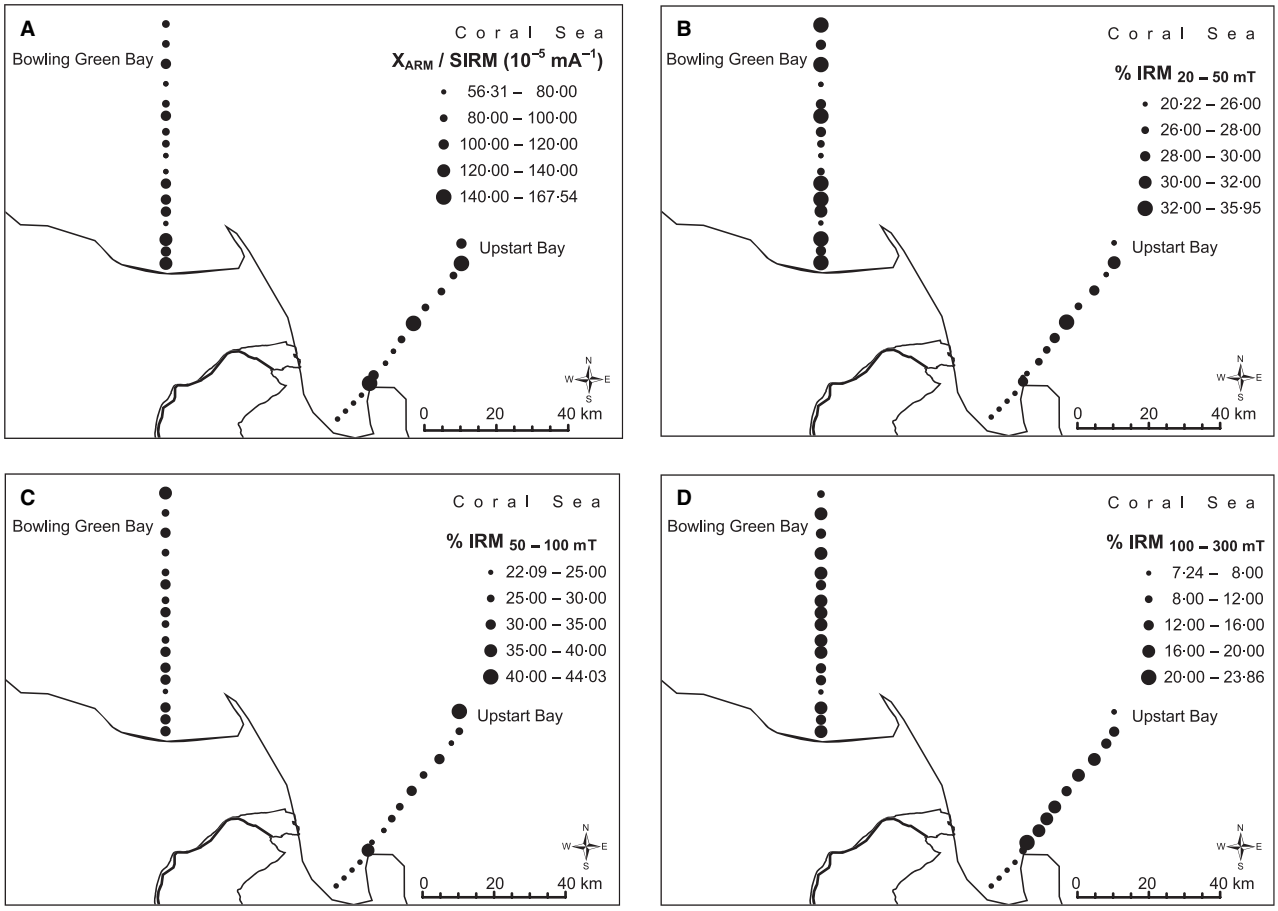

Fig. 10. Magnetic concentration and magnetic grain-size parameters for inclusions within the medium sand fraction of the offshore grab samples.

(based upon excess ^{210}Pb core profiles; Orpin *et al.*, 2004). There is also the possibility in Upstart Bay (and in western Bowling Green Bay) of surface sediment having mixed with sediment as much as 7000 years in age, because of low sedimentation rates in these areas. Such mixing would be very unlikely in eastern Bowling Green Bay because of the extremely high rates of sediment aggradation recorded from there (Orpin *et al.*, 2004).

Comparison of offshore grab sands with the Burdekin River bed samples

To investigate any relationships between the sands transported by the different tributaries of the Burdekin system and the offshore sands, cluster analysis was run on a combined onshore and offshore magnetic inclusions data set, using four magnetic parameters: the saturation remanence (SIRM), indicating magnetic concentration; the ultrafine magnetite indicator (χ_{ARM}/SIRM); and two remanence ratios (%$IRM_{20–50mT}$, %$IRM_{50–100mT}$). These variables were selected as they provide the most discrimination between the grab samples. Statistical indicators of cluster performance indicate that the 'best' solution is obtained with eight clusters. In the non-linear map, the clusters appear reasonably well-separated, with the exception of Cluster Three (Fig. 11). Cluster One, consisting only of Upper Burdekin River samples from Brigalow and Big Bend, has the lowest ultrafine magnetite (χ_{ARM}/SIRM) value of any cluster (Table 4). The rest of the Brigalow and Big Bend samples plot in Cluster Two, together with one of the Upstart Bay, grab samples. Cluster Two has the highest %$IRM_{50–100mT}$ value and a slightly higher χ_{ARM}/SIRM than Cluster One. Cluster Three (three Upstart Bay, grab samples and the Reid River sample) has a wider distribution in the two-dimensional statistical map. It has the highest concentration of magnetic minerals (having the highest SIRM) but the lowest %$IRM_{20–50mT}$ value.

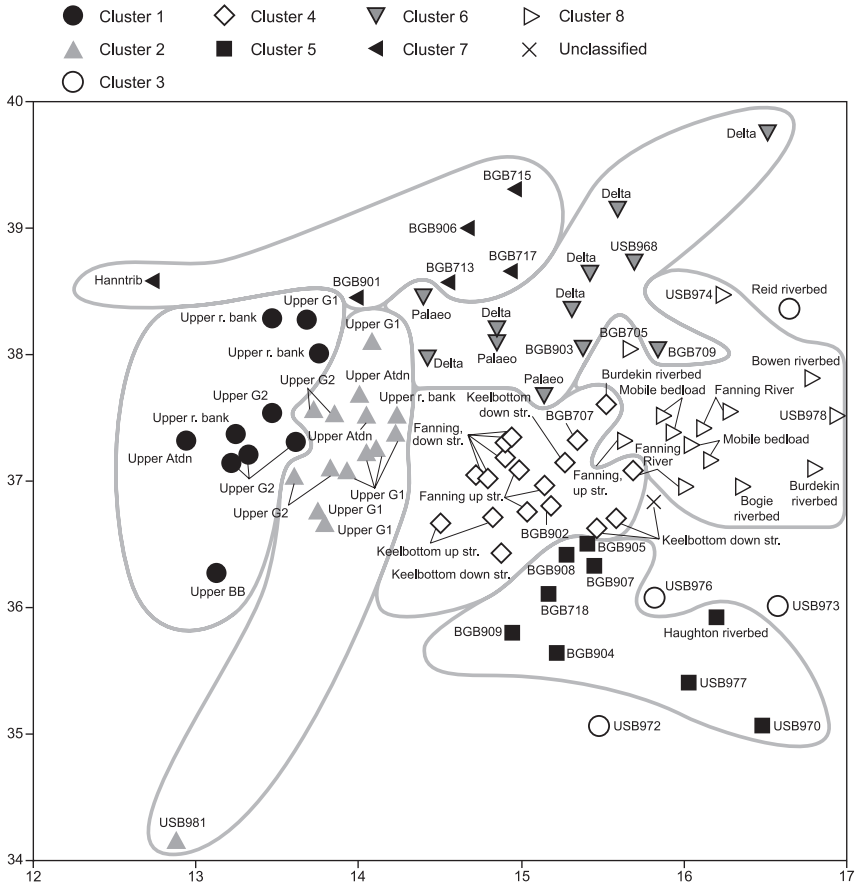

Fig. 11. Non-linear map of the five-cluster solution for the combined Burdekin River and offshore sand-fraction inclusion data set (BGB, Bowling Green Bay; USB, Upstart Bay; river samples as in Fig. 1 caption).

Table 4. Parameter means for the eight-cluster solution, combined Burdekin River sand and offshore sand (magnetic inclusion) data set.

	Cluster 1	Cluster 2	Cluster 3	Cluster 4	Cluster 5	Cluster 6	Cluster 7	Cluster 8
χ_{ARM}/SIRM (10^{-5} A m^{-1})	51·26	70·39	79·90	85·22	85·94	98·51	103·80	121·30
%IRM$_{20-50mT}$	30·57	29·26	28·96	29·42	26·39	32·90	32·95	30·79
%IRM$_{50-100mT}$	35·28	35·70	29·08	28·98	26·49	33·95	33·26	27·99
SIRM (10^{-6} A m^2 kg^{-1})	159·70	152·00	445·10	166·40	275·20	247·50	105·10	213·90

Cluster Four is a small cluster in the centre of the map, consisting of the Fanning and Keelbottom confluence samples and two Bowling Green Bay, grab samples. It has moderate values for all of the magnetic parameters. Cluster Five consists of six Bowling Green Bay and two Upstart Bay, grab samples and the Haughton River sample. Cluster Six has moderate to high parameter values and consists of two Bowling Green Bay and one Upstart Bay, grab samples and the majority of the palaeo-channel and delta samples. Cluster Seven has the lowest magnetic concentration (i.e. the lowest SIRM) and the highest %IRM$_{20-50mT}$ value, and comprises five Bowling Green Bay, grab samples and the Hann Creek sample. The remaining cluster, Eight, contains two Upstart Bay, grab samples and one from Bowling Green Bay together with the Bowen, Fanning and Burdekin riverbed samples and the Burdekin mobile bedload samples (collected on the delta in 2000). It has the highest ultrafine magnetite (χ_{ARM}/SIRM) value of any of the clusters.

The geographic distribution of these identified clusters along the two cross-shelf transects is quite varied (Fig. 12). Samples in Bowling Green Bay belong to one of five different clusters. The mid-transect samples belong to one of two clusters which appear related to the Haughton River or Hann Creek. The samples in Upstart Bay show affinity with five different clusters.

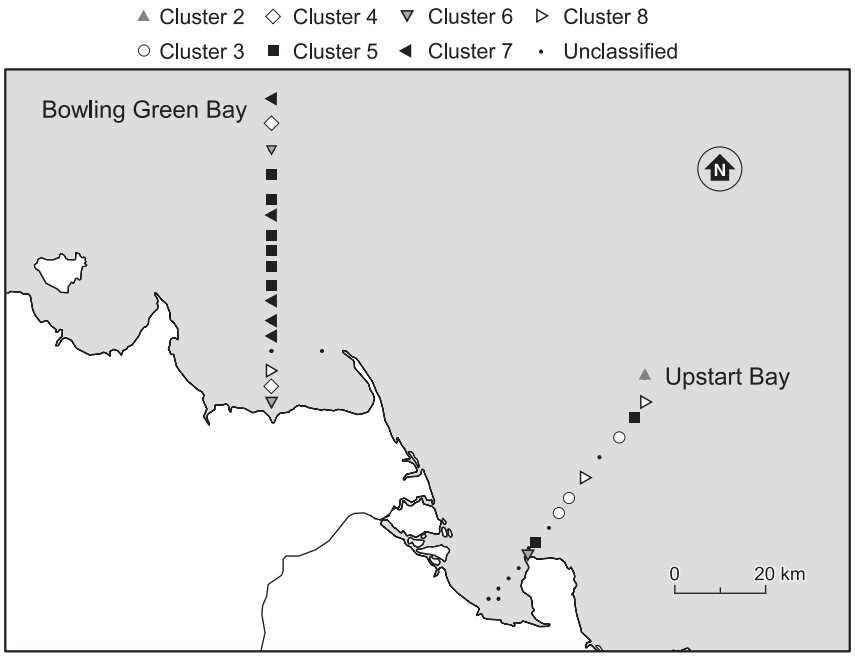

Fig. 12. Spatial distribution of clusters in Bowling Green Bay and Upstart Bay for the combined Burdekin River sand and offshore sand-fraction inclusion data set.

DISCUSSION

One of the key aims here was to identify whether sediment sourcing in the large, complex catchment of the Burdekin River could be achieved by magnetic fingerprinting. Magnetic inclusion-based data from the medium sand fraction of samples from the Burdekin River indicate that sediments collected from the different subcatchments and reaches of the Burdekin catchment display robustly different magnetic properties (Fig. 8). The Upper Burdekin samples from Brigalow and Big Bends mainly fall into one, well-defined statistical cluster (Five). This cluster is distinct from samples collected from the Upper Burdekin River upstream and downstream of the Keelbottom Creek and Fanning River confluences (Cluster Two), which, in turn, are distinct from the samples collected from the Fanning River itself. Samples from Hann Creek (Cluster Three), which drains a different region and geology to the Fanning River and Keelbottom Creek, are also magnetically distinct from other samples in this region. This distinction demonstrates that magnetic discrimination of present-day river sediments is possible at quite high spatial resolution. Given the distinctly different magnetic character of samples taken at one site on the delta from floods in subsequent years, and given that the samples from the Big and Brigalow Bend sites were collected a few years earlier than those from the other sites, it is possible that some of the difference between the groups is also influenced by transport and deposition of sediment by large, individual flood events from discrete subcatchment areas (see below).

Noting that significant volumes of sand are transported in suspension during high flow events, the upper north-western Burdekin River subcatchments have been thought to be a major source of sediment to the delta and further offshore. Here, however, the new magnetic data indicate that other sand inputs may contribute significantly. For example, only those samples collected from the Burdekin delta during the flood events in 1998 and 1999 belong to the same cluster (Four) as some of the Upper Burdekin River samples. In contrast, samples collected in the 2000 flood event belong to a different cluster (One), suggesting that the sediment in suspension in the channel at the time of sampling of this event derived from a different source. Possible Cluster One source matches include sediments from other subcatchments (the Bowen, Bogie and Fanning). Hydrographs from gauging stations throughout the catchment (see, e.g. Amos *et al.*, 2004; Fig. 4) demonstrate that in the 2000 event, discharge occurred in many of the tributaries and consequently flood water (and suspended sediment) from different parts of the catchment would have arrived at the sampling point at the delta at different times. The medium sand fraction of the mobile bedload samples in the lower Burdekin River in 2000 also clusters with the Fanning, Bowen and Bogie River samples. The most probable explanation for the difference between the

2000 samples and those from the 1998 and 1999 flood events is that the 2000 event medium sand was derived largely from the Bowen and Bogie catchments (below the Burdekin Falls Dam) while the earlier events transported medium sand from areas upstream of the Falls Dam. Within the Burdekin catchment, sediments are mobilized from different subcatchments by runoff generated by intense, spatially localized rainfall events. The 1998 flood resulted from rain mostly in the Upper Burdekin catchment and runoff was sufficient to fill Dalrymple Lake and continue to the coast as a substantial flood wave (peaking at 11 904 m^3 sec^{-1}), evidently transporting medium sand through the system. In contrast, the discharge in the 1999 event was relatively small (peak flow at Clare was 1214 m^3 sec^{-1}) and is unlikely to have transported sand so efficiently (and notably not through Dalrymple Lake). In this event, the medium sand below the dam is likely to have been derived by reworking of sediment deposited by the antecedent (1998) event. That the 1998 and 1999 sediments belong to the same cluster (Four) as some of the Upper Burdekin River confirms previous observations that construction of the Falls Dam is not preventing suspended sediment from the upper catchments reaching the delta.

It is also notable that a number of the offshore samples have, as yet, no magnetically matching source. While caution is needed at this pilot stage, given the small number of river subcatchment and marine sand samples presently characterized, the magnetic data suggest that the source(s) of the offshore non-carbonate medium sand may not be related to the modern Burdekin River sediment supply. Similarly, the modelling output from the Prosser *et al.* (2002) study indicated that much of the Burdekin catchment may contribute little to offshore export of sediment because of its distal nature, with many opportunities for redeposition of eroded sediment along its transport path. Conversely, the results of Prosser *et al.* suggest that higher rates of sediment delivery might typify the more coastal catchments, with their reduced transport length. An additional possibility is that the offshore sand represents a relict and alongshore mobile sand, as described by Larcombe & Carter (2004). Further sampling and analysis are required to test the magnetic evidence of an onshore/offshore sediment mismatch; as yet, for example, no samples have been obtained from the Belyando River, or from the Suttor or Star subcatchments.

During the Quaternary, there have been significant changes in the drainage paths of the Burdekin (e.g. Belperio, 1983; Fielding *et al.*, 2003). The palaeo-channel samples measured here appear magnetically similar to modern-day samples, belonging to the same cluster (Four) as some Upper Burdekin River samples and the 1998 and 1999 flood event (delta) samples. Even if changes in channel geography have occurred, the palaeo-channels may have obtained their sediment from the same source magnetic area (i.e. the same geology and soil type) as the modern channels.

Magnetic discrimination of sources can be improved by applying this approach to a comprehensive set of samples from additional regions of the Burdekin catchment and from the coastal river catchments. It is both possible and useful to extend this inclusion-based method of magnetic 'fingerprinting' to other potential source areas, and other (finer) particle sizes, to identify sediment source signatures and their affinity with the offshore sedimentary record, and examine changes in sediment source, both at the present day and through the historical and geological past.

CONCLUSIONS

It appears feasible to achieve magnetic differentiation of Burdekin River sediment sources at the subcatchment scale. Sands sampled from different tributaries within the Burdekin catchment can be differentiated on the basis of the magnetic properties of inclusions within their host silicate grains. Magnetic methods thus provide a means for discrimination of sediment sources. Magnetic analysis of untreated sediment fractions can be used to indicate sediment provenance, for large numbers of samples (e.g. hundreds). However, use of a magnetic inclusion-based data set (e.g. for selected representative subsets of samples), rather than an untreated magnetic data set, removes any possible influence of post-depositional or hydraulic sorting processes which might otherwise obscure or confound the primary provenance patterns.

This magnetic discrimination appears to be possible at high spatial resolution as riverbed samples from a relatively small part of the Burdekin catchment (i.e. the north-western Upper Burdekin River, the Burdekin confluences with Keelbottom Creek, the Fanning River and Hann Creek) have magnetic properties which belong to statistically different cluster groups.

It seems possible to identify sediment provenance associated with large individual flood events. Suspended sand samples collected from

the Burdekin River on the delta during flood events in 1998, 1999 and 2000, and the medium sand fraction from the mobile bedload in 2000, identify a different source for the 2000 sand than for the 1998 and 1999 sand. The latter events appear to have an Upper Burdekin River source while the medium sand moving in the lower Burdekin River in 2000 was from the Bowen and Bogie subcatchments. The flashy discharge behaviour of the Burdekin, associated with intense and spatially localized rainfall events, may be a key factor in enabling greater discrimination of source areas than might be possible in a more perennial discharge system.

The medium sand fractions of the surface sediments in Upstart Bay and Bowling Green Bay are magnetically distinct, suggesting that the sand sources for the two bays have been different for the timespan encompassed by the grab sampling process. Some of the offshore medium sands have no statistical affinity with any of the fluvial sources examined here. Offshore, local headland and/or as yet unsampled fluvial sources may contribute to these different offshore magnetic signatures.

ACKNOWLEDGEMENTS

Financial support from the Royal Society (through a Royal Society-Wolfson Research Award to BAM), NERC (UK), and the Australian Research Council is gratefully acknowledged. We thank Jon Brodie for collection of some of the river catchment samples. We thank Jon Cox and Emlyn Wright for sample preparation and carrying out many of the magnetic measurements. Irena Zagorskis, Ken Woolfe and Alan Orpin assisted in collection of the offshore samples. The two reviewers are thanked for their incisive and helpful reviews.

REFERENCES

Alekseeva, V.A. and **Hounslow, M.W.** (2004) Clastic sediment source characterization using discrete and included magnetic properties – their relationship to conventional petrographic methods in early Pleistocene fluvial-glacial sediments, Upper Don River Basin (Russia). *Phys. Chem. Earth*, **29,** 961–971.

Alexander, J. and **Fielding, C.R.** (1997) Gravel antidunes in the tropical Burdekin River, Queensland, Australia. *Sedimentology*, **44,** 327–337.

Alexander, J. and **Fielding, C.R.** (2006) Coarse-grained floodplain deposits in the seasonal tropics: towards a better facies model. *J. Sed. Res.*, **76,** 539–556.

Alexander, J., Fielding, C.R. and **Pocock, G.D.** (1999) Flood behaviour of the Burdekin River, Tropical North Queensland, Australia. In: *Floodplains: Interdisciplinary Approaches* (Eds J. Alexander and S. Marriott), *Geol. Soc. London Spec. Publ.*, **163,** 27–40.

Alexander, J., Fielding, C.R., Wakefield, S.J., George, M.T. and **Cottnam, C.F.** (2001) Fluvial geochemistry through a short-duration, tropical-cyclone induced discharge event in the Burdekin River and Hann Creek, North Queensland, Australia. *Aquat. Geochem.*, **7,** 275–293.

Alibert, C., Kinsley, L., Fallon, S.J., McCulloch, M.T., Berkelmans, R. and **McAllister, F.** (2003) Source of trace element variability in Great Barrier Reef corals affected by the Burdekin flood plumes. *Geochim. Cosmochim. Acta*, **67,** 231–246.

Amos, K.J., Alexander, J., Horn, A., Pocock, G.D. and **Fielding, C.R.** (2004) Supply limited sediment transport in a high-discharge event of the tropical Burdekin River, North Queensland, Australia. *Sedimentology*, **51,** 145–162.

Bazylinksi, D.A. (1990) Anaerobic production of single-domain magnetite by the marine magnetotactic bacterium, strain MV-1. In: *Iron Biominerals* (Eds R.B. Frankel and R.P. Blakemore), pp. 69–77, Plenum Press, New York.

Belperio, A.P. (1979) The combined use of wash load and bed material load rating curves for the calculation of total load, an example from the Burdekin River, Australia. *Catena*, **6,** 317–329.

Belperio, A.P. (1983) Terrigenous sedimentation in the Central Great Barrier Reef lagoon, a model from the Burdekin Region. *BMR J. Aust. Geol. Geophys.*, **8,** 179–190.

Blakemore, R.P., Short, K.A., Bazylinksi, D.A., Rosenblatt, C. and **Frankel, R.B.** (1984) Microaerobic conditions are required for magnetite formation within *Aquasprillum magnetotacticum*. *Geomicrobiol. J.*, **4,** 53–71.

Brodie, J. (1996) River flood plumes in the Great Barrier Reef lagoon. In: Great Barrier Reef, Terrigenous Sediment Flux and Human Impacts. Eds P. Larcombe, K.J. Woolfe and R. Purdon), pp. 33–39. CRC Reef Research Centre, Townsville.

Caitcheon, G.G. (1998a) The significance of various sediment magnetic mineral fractions for tracing sediment sources in Killimicat Creek. *Catena*, **32,** 131–142.

Caitcheon, G.G. (1998b) The application of environmental magnetism to sediment source tracing, a new approach. CSIRO Land and Water Technical Report No. 21/98, 133 pp.

Cavanagh, J.E., Burns, K.A., Brunskill, G.J. and **Coventry, R.J.** (1999) Organochlorine pesticide residues in soils and sediments of the Herbert and Burdekin River regions, North Queensland – implications for contamination of the Great Barrier Reef. *Mar. Pollut. Bull.*, **39,** 367–375.

Dekkers, M.J., Langereis, C.G., Vriend, S.P., van Santvoort, P.J.M. and **de Lange, G.J.** (1994) Fuzzy c-means cluster analysis of early diagenetic effects on natural remanent magnetisation acquisition in a 1.1 Myr piston core from the Central Mediterranean. *Phys. Earth Planet. In.*, **85,** 155–171.

Fielding, C.R. and **Alexander, J.** (1996) Sedimentology of the Upper Burdekin River of North Queensland, Australia – an example of a tropical, variable discharge river. *Terra Nova*, **8,** 447–457.

Fielding, C.R., Alexander, J. and **McDonald, R.** (1999) Sedimentary facies from GPR surveys of the modern, upper Burdekin River of north Queensland, Australia: consequences of extreme discharge fluctuations. In: (Eds N.D. Smith and J. Rogers), *Current Research in Fluvial Sedimentology*, International Association of Sedimentologists Special Publication, London, **28,** 347–362.

Fielding, C.R., Trueman, J.D., Dickens, G.R. and **Page, M.** (2003) Anatomy of the buried Burdekin River channel across the Great Barrier Reef shelf, how does a major river

operate on a tropical mixed siliciclastic/carbonate margin during sea level lowstand? *Sed. Geol.*, **157,** 291–301.

Fielding, C.R., Trueman, J.D. and **Alexander, J.** (2005) Sedimentology of the Modern and Holocene Burdekin River Delta of North Queensland, Australia – controlled by river output, not by waves and tides. In: *Deltas, New and Old* (Eds L. Giosan and J. Bhattacharya), *SEPM Spec. Publ.*, **83,** 467–496.

Fielding, C.R., Trueman, J.D. and **Alexander, J.** (2006) Holocene depositional history of the Burdekin delta of northeastern Australia: a model for a low accommodation, highstand delta. *J. Sed. Res.*, **76,** 411–428.

Furnas, M.J. (2003) *Catchments and Corals: Terrestrial Runoff to the Great Barrier Reef*. Australian Institute of Marine Science and Reef CRC, Townsville, 353 pp.

Hanesch, M., Scholger, R. and **Dekkers, M.J.** (2001) The applications of fuzzy c-means cluster analysis and nonlinear mapping to a soil data set for the detection of polluted sites. *Phys. Chem. Earth*, **26,** 885–891.

Hounslow, M.W. and **Maher, B.A.** (1996) Quantitative extraction and analysis of carriers of magnetisation in sediments. *Geophy. J. Internat.*, **124,** 57–74.

Hounslow, M.W. and **Morton, A.C.** (2004) Evaluation of sediment provenance using magnetic mineral inclusions in clastic silicates, comparison with heavy mineral analysis. *Sed. Geol.*, **171,** 13–36.

Johnson, D. (1996) Knowledge summary of terrigenous input to the Central Great Barrier Reef. In: *Great Barrier Reef, Terrigenous Sediment Flux and Human Impacts* (Eds P. Larcombe, K.J. Woolfe and R. Purdon), pp. 86–91. CRC Reef Research Centre, Townsville.

Karlin, R.A. and **Levi, S.** (1985) Geochemical and sedimentological control of the magnetic properties of hemipelagic sediments. *J.* Geophys. Res., **90,** 10373–10392.

Kruiver, P.P., Kok, Y.S., Dekkers, M.J., Langereis, C.G. and **Laj, C.** (1999) A pseudo-Thellier relative palaeointensity record, and rock magnetic and geochemical parameters in relation to climate during the last 276 kyr in the Azores region. *Geophys. J. Int.*, **136,** 757–770.

Larcombe, P. and **Carter, R.M.** (2004) Cyclone pumping, sediment partitioning and the development of the Great Barrier Reef shelf system, a review. *Quatern. Sci. Rev.*, **23,** 107–135.

Larcombe, P. and **Woolfe, K.J.** (1999) Increased sediment supply to the Great Barrier Reef will not increase sediment accumulation at most coral reefs. *Coral Reefs*, **18,** 163–169.

Larcombe, P., Woolfe, K.J., Amjad, N., Barnes, D.J., Brodie, J., Brunskill, G.J., Bryce, S., Carter, R.M., Costen, A., Crook, K.A.W., Crossland, C., Deacon, G.L., Ferland, M.A., Gorrie, A., Grindrod, J., Johnson, D.P., McIntyre, C., Neil, D.T., Okubo, C., Orpin, A.R., Purdon, R.G., Pye, K., Ridd, P.V., Shulmeister, J., Taylor, J. and **Walker, G.S.** (1996) Terrigenous sediment fluxes and the central Great Barrier Reef shelf, the current state of knowledge. In: *Great Barrier Reef, Terrigenous Sediment Flux and Human Impacts* (Eds P. Larcombe, K.J. Woolfe and R. Purdon), pp. 7–23. CRC Reef Research Centre, Townsville.

Maher, B.A., Thompson, R. and **Hounslow, M.W.** (1999) Introduction to Quaternary Climates, Environments and Magnetism. In: *Quaternary Climates, Environments and Magnetism* (Eds B.A. Maher and R. Thompson), pp. 1–48. Cambridge University Press, Cambridge, UK.

Moss, A.J., Rayment, G.E., Reilly, N. and **Best, E.K.** (1992) *A Preliminary Assessment of Sediment and Nutrient Exports from Queensland Coastal Catchments*, Queensland Department of Environment and Heritage, Technical Report 5, Brisbane, Queensland Government, 27p.

Nakayama, K., Fielding, C.R. and **Alexander, J.** (2002) Variations in character and preservation potential of vegetation-induced obstacle marks in the variable discharge Burdekin River of north Queensland, Australia. *Sed. Geol.*, **149,** 199–218.

Neil, D.T., Orpin, A.R., Ridd, P.V. and **Yu, B.** (2002) Sediment yield and impacts from river catchments to the Great Barrier Reef lagoon. *Aust. J. Mar. Freshwat. Res.*, **53,** 733–752.

Oldfield, F., Rummery, T.A., Thompson, R. and **Walling, D.E.** (1979) Identification of suspended sediment sources by means of magnetic measurements. *Water Resour. Res.*, **15,** 211–218.

Oldfield, F., Maher, B.A., Donoghue, J. and **Pierce, J.** (1985) Particle-size related, mineral magnetic source sediment linkages in the Rhode River catchment, Maryland, USA. *J. Geol. Soc.*, **142,** 1035–1046.

Orpin, A.R. and **Ridd, P.V.** (1996) Sediment distribution and transport mechanisms, Burdekin region, central Great Barrier Reef lagoon. In: *Great Barrier Reef, Terrigenous Sediment Flux and Human Impacts* (Eds P. Larcombe, K.J. Woolfe and R. Purdon), pp. 128–143. CRC Reef Research Centre, Townsville.

Orpin, A.R., Ridd, P.V. and **Stewart, L.K.** (1999) Assessment of the relative importance of major sediment-transport mechanisms in the central Great Barrier Reef. *Aust. J. Earth Sci.*, **46,** 883–896.

Orpin, A.R., Brunskill, G.J., Zagorskis, I. and **Woolfe, K.J.** (2004) Patterns of mixed siliciclastic-carbonate sedimentation adjacent to a large dry-tropics river on the central Great Barrier Reef shelf, Australia. *Aust. J. Earth Sci.*, **51,** 665–683.

Pringle, A.W. (2000) Evolution of the east Burdekin Delta coast, Queensland, Australia 1980-1995. *Z. Geomorph. N. F.*, **44,** 273–304.

Prosser, I.P., Moran, C.J., Lu, H., Scott, A., Rustomji, P., Stevenson, J., Priestly, G., Roth, C.H. and **Post, D.** (2002) Regional patterns of erosion and sediment transport in the Burdekin River catchment. CSIRO Land and Water, Technical Report 5/02, pp 44.

Schmidt, A.M., von Dobeneck, T. and **Bleil, U.** (1999) Magnetic characterisation of Holocene sedimentation in the South Atlantic. *Paleoceanography*, **14,** 465–481.

Vriend, S.P., van Gaans, P.F.M., Middelburg, J. and **de Nus, A.** (1988) The application of fuzzy c-means cluster analysis and non-linear mapping to geochemical datasets, examples from Portugal. *Appl. Geochem.*, **3,** 213–224.

Walden, J., Slattery, M.C. and **Burt, T.P.** (1997) Use of mineral magnetic measurements to fingerprint suspended sediment sources, approaches and techniques for data analysis. *J. Hydrol.*, **202,** 353–372.

Walling, D.E. and **Woodward, J.C.** (1995) Tracing sources of suspended sediment in river basins – a case-study of the River Culm, Devon, UK. *Marine Freshw. Res.* **46,** 327–336.

Walling, D.E., Peart, M.R., Oldfield, F. and **Thompson, R.** (1979) Suspended sediment sources identified by magnetic measurements. *Nature* **281,** 110–113.

Watkins, S.J. and **Maher, B.A.** (2003) Magnetic characterisation of present-day deep-sea sediments and sources in the North Atlantic. *Earth Planet. Sci. Lett.*, **214,** 379–394.

Wolanski, E. (1994) *Physical Oceanographic Processes of the Great Barrier Reef*. CRC Press, Boca Raton, FL, 194 pp.

Manuscript received 18 January 2008; revision accepted 11 July 2008

APPENDIX

Magnetic measurements

Low (χ_{lf}, 0·47 kHz) and high (χ_{hf}, 4·7 kHz) frequency magnetic susceptibility were measured using a Bartington MS2 dual-frequency sensor (Bartington Instruments Ltd, Witney, UK). Anhysteretic remanent magnetization (ARM) was imparted to samples using a Molspin AF demagnetizer with a peak A.F. of 85 mT with a superimposed DC field of 0·08 mT and measured using a Molspin magnetometer. The ARM is expressed here as a mass-specific susceptibility of ARM (χ_{ARM}) by normalizing with the DC field. The ARMs were then demagnetized before growing isothermal remanent magnetizations (IRMs) at six successive steps (10, 20, 50, 100, 300 and 1000 mT), which were measured using a Molspin magnetometer. Fields up to 300 mT were imparted using a pulse magnetizer and the 1000 mT ('saturation' field) using a Highmoor DC electromagnet (Highmoor Electronics Ltd, Salford, UK).